JOURNAL OF MATERIALS SCIENCE 30 (1995) 5394–5398

Energetically evaluated load-indentation measurements of different classes of material

B. ROTHER
Forschungsinstitut für Edelmetalle und Metallchemie, Katharinenstrasse 17, D-73525 Schwäbisch Gmünd, Germany

Alumina, acryl glass, colour paint and India-rubber have been investigated by load–indentation measurements. The data were evaluated in terms of specific deformation energy densities and in terms of the conventional hardness under load. The specific energy densities were found to indicate a constant material response to the penetration of the indentor for extended penetration depth ranges. However, the conventionally calculated hardness values show a typical decrease for increased penetration depth.

1. Introduction

Load–indentation measurements are widely used for hardness measurements with loads in the range of about 0.1–1000 mN. The corresponding penetration depth range is material- and indentor-dependent and can be expected to be between some tens of nanometres and some tens of micrometres. The measurement principle permits the calculation of hardness under load (universal hardness, HU) as the ratio of load to contact area between the indentor and the probed material. Thereby, the calculation of the contact area from the penetration depth is the most critical point of the procedure. A variety of different mechanisms including shape deviations of the indentor and specific response characteristics of the probed material, are generally acknowledged to be responsible for the decrease of the HU values at increasing penetration depths [1–3]. The nature and mathematical balance of these mechanisms, which are summarized in the term "indentation size effect" (ISE), have been the subject of extensive investigations [1, 3–6]. Suggested corrections of the HU values are, however, dependent on the accuracy of the physical model and of the calibration procedure. The correction parameters are generally only valid for each similar material category [3, 7].

A recently reported energy-related interpretation of load–indentation measurements has been shown to avoid the above-mentioned problems for hard materials such as silicon single crystal, steel, glass and hard coatings [8, 9]. The present paper aims to demonstrate the suitability of the approach also to the investigation of ceramics, plastics, paints and rubber.

2. The energy-related interpretation of load–indentation measurements

The applied approach aims to calculate two specific energy densities into which the energy, W_i, of the penetrating indentor is distributed within the probed material [8]. Thereby, a volume-related (index V) and an area-related (index A) energy term are considered. The energy balance thus reads

$$W_i = \overline{w_V} k_V s^3 + \overline{w_A} k_A s^2 = e_V s^3 + e_A s^2 \quad (1)$$

with the mean energy densities $\overline{w_V}$ and $\overline{w_A}$, the shape factors k_V and k_A, as well as the penetration depth, s. Equation 1 starts from the existence of mean energy densities as well as from a linear relation between the penetration depth and the dimension of the energy densification zone under the penetrating indentor. For different penetration depths different e_V and e_A values can be expected. Proof for Equation 1, for at least limited penetration depths, follows from the appearance of linear ranges in the first derivative of the load in relation to the penetration depth, s (differential load feed, DLF) which is identical to the second derivative of the energy in relation to s.

The two specific densities, e_V and e_A, can thus directly be calculated from the load–indentation data. Constant e_V and e_A values of linear DLF ranges are considered as a proof of a constant resistance of the probed material against the penetration of the indentor over the corresponding penetration range. Homogeneous materials have been shown to exhibit that behaviour which is illustrated by two selected DLF plots shown in Fig. 1a. For comparison, Fig. 1b illustrates the corresponding HU data. Contrary to the constant material response documented by the constant energy densities in Fig. 1a, the HU values of Fig. 1b show a typical decrease with increasing penetration depth. A comparison of coefficients between the DLF formulas and the conventional hardness formula indicates the comparability of e_V and the universal hardness HU. Therefore, for e_V the term hardness equivalent was suggested [8].

Promising results of DLF analysis have been obtained for the following problems:
Minimization of ISE [9], comparability of different measurement devices [10], comparability of Vickers

0022–2461

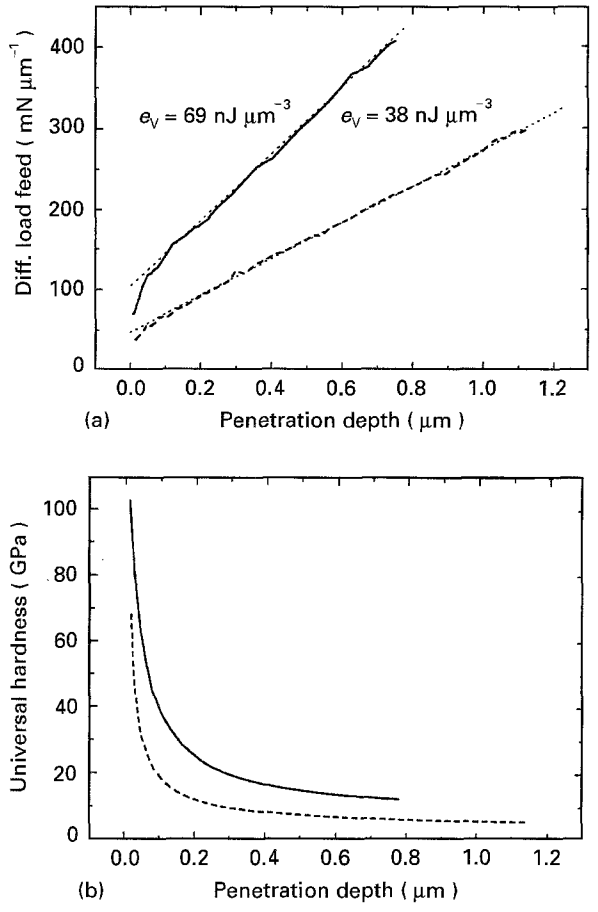

Figure 1 Load–indentation results of (——) polished hardened high-speed steel and (– – –) glass. (a) DLF plots, (b) HU plots. (-----) Regression lines.

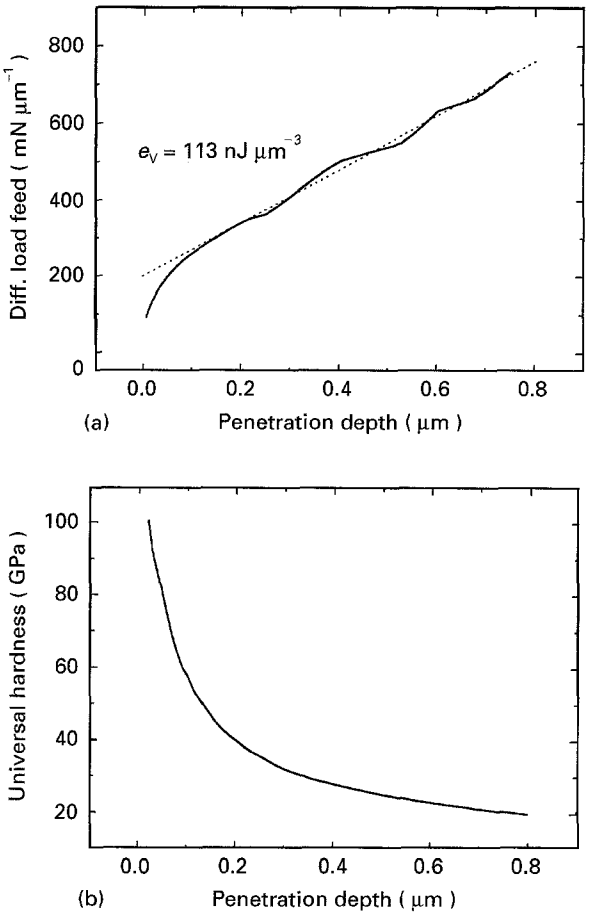

Figure 2 Load–indentation results of hipped and polished alumina, end load 340 mN. (a) DLF plot, (b) HU plot. (-----) Regression line.

and Berkovich results [10], and measurements on rough surfaces [11].

A particular importance could be proved for coating–substrate composites by the potential of the approach to separation between coating and substrate properties [8, 12], evaluation of the interface strength [12–14], and qualitative estimation of intrinsic coating stresses [10].

Owing to recent results, the two specific energy densities, e_V and e_A, can be expected to characterize the indentor specific resistance of the probed material against plastic and elastic deformation, respectively [15].

3. Experimental procedure

The load–indentation measurements were performed with a commercially available depth-sensing hardness measurement device which is characterized by a load range of 0.4–1000 mN, a load resolution of 0.02 mN, an indentor shift resolution of 2 nm, a stepwise load increment with adjustable waiting period between the steps, with quadratic increase of step height.

The device was equipped with a Vickers indentor. Mechanically pressed and polished alumina, acryl glass, colour paint and India-rubber were used as sample materials.

Prior to indentation experiments the indentor was cleaned and two unrecorded indentation runs were performed. In the following, five individual load–indentation measurements were recorded, averaged and numerically differentiated. A specially developed averaging and smoothing procedure [16] was applied.

4. Results

4.1. DLF results

Identical load–indentation data of the individual sample materials were used for DLF as well as for conventional hardness calculation. Plots of the results versus penetration depth are shown in Figs 2–5.

The most critical material for the indentation experiments was found to be the alumina, which is attributed to its mean surface roughness of R_z = 8.9 µm and its granular nature. Reproducible load–indentation data could only be obtained for penetration depths between 0.2 and 0.8 µm. In that range the calculated DLF plots show only slight tooth-like deviations from the averaged regression line (Fig. 2a). At increased penetration depth, intense and irregular scattering of the DLF data indicates fracture events. On the contrary, the averaged HU plots also show a regular behaviour at increased penetration depths (Fig. 2b).

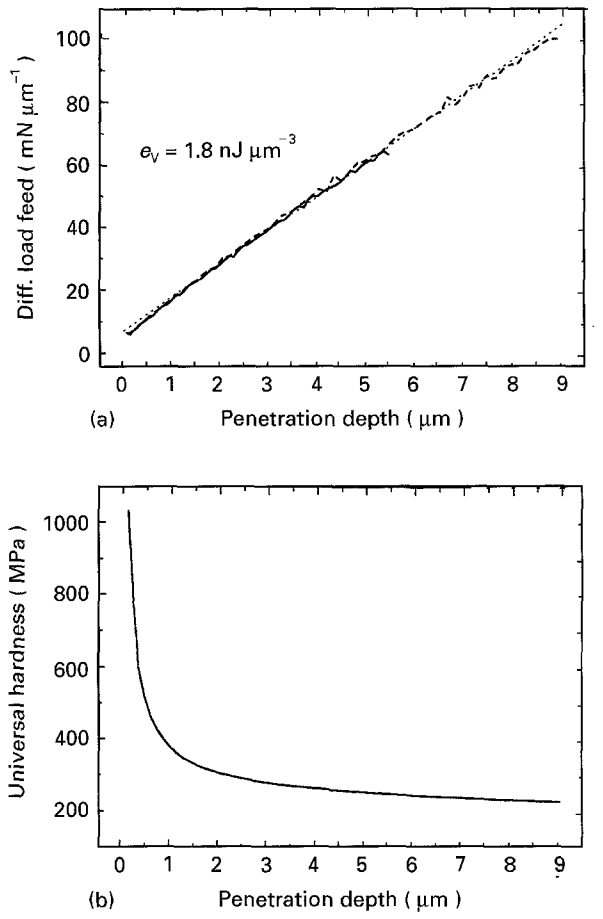

Figure 3 Load–indentation results of acryl glass. (a) DLF plot, (——) end load 200 mN, (– – –) end load 500 mN, (- - - -) regression line; (b) HU plot. (——) end load 500 mN.

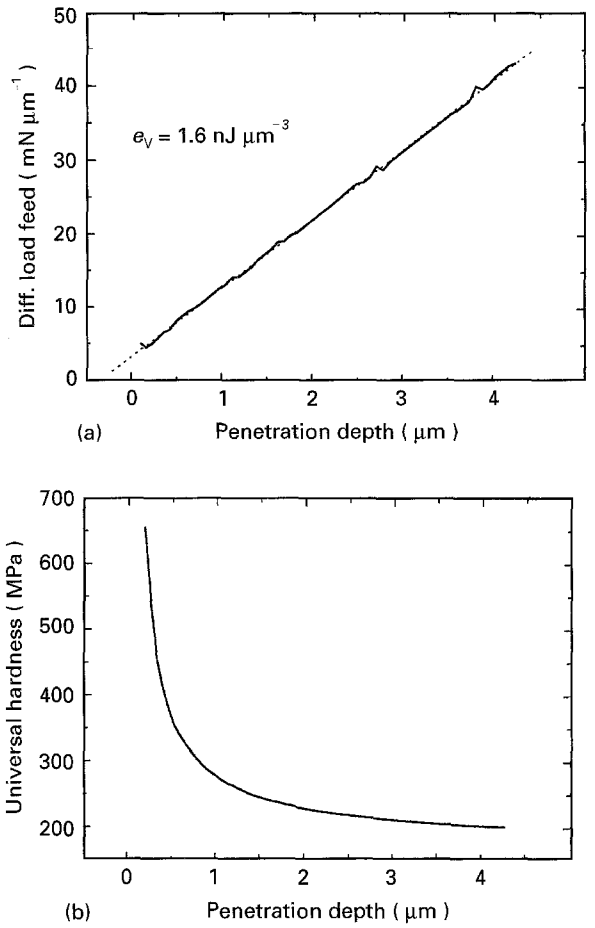

Figure 4 Load–indentation results of colour paint, 60 µm thick, end load 100 mN (a) DLF plot, (- - - -) regression line; (b) HU plot.

The other sample materials exhibited reproducible load–indentation behaviour over extended penetration depth ranges. As an example, the DLF plots shown in Fig. 3a illustrate the coincidence of the linear ranges for different end loads. In all DLF plots shown in Figs 2a, 3a, 4a and 5a, extended linear ranges can be evaluated in terms of the slope-related hardness equivalent, e_v. The corresponding values are indicated in the figures.

4.2. HU results

All HU plots shown in Figs 2b, 3b, 4b and 5b exhibit the well-known decrease with increasing penetration depth. This typical behaviour also appears for the differing penetration depth ranges of the different materials. As an example, the decrease of the HU values by a factor of two or three is summarized for the individual materials by the data given in Table I.

5. Discussion

5.1. DLF results

The DLF plots of the investigated materials prove the existence of extended linear ranges, as already demonstrated in connection with other materials [8, 9]. The charge involved in the deformation processes involved in Equation 1 is thus confirmed. Obviously, the specific deformation energies, e_V and e_A, remain constant for the linear ranges, which indicates a constant resistance of the probed material against the penetration of another.

Tooth-like deviations from the total regression line, as they appear in the DLF plot of alumina (Fig. 2b), indicate the existence of successively changing response characters, as can be expected for deformations of the individual powder particles alternating with shifts of the particles against each other. A closer treatment of the effects will be the subject of further investigations. The non-linear DLF plot behaviour for alumina and rubber at low penetration depths is also not a subject of the present investigations.

5.2. HU results

Contrary to the DLF results, the HU plots indicate a considerable decrease for increasing penetration depths. The nature of that behaviour is attributed to a combination of several mechanisms, the effects of which are summarized by the term "indentation size effect" (ISE). For investigations of hard material with low loads and, consequently, low penetration depth ranges up to about 1 µm, the HU decrease is usually corrected by considering tip rounding of the indentor [1, 3, 4]. The general principle of these procedures is the definition of a specific rounding shape of pyramidal or conical indentors and to calculate an expected real contact area, A_r, between the sample and

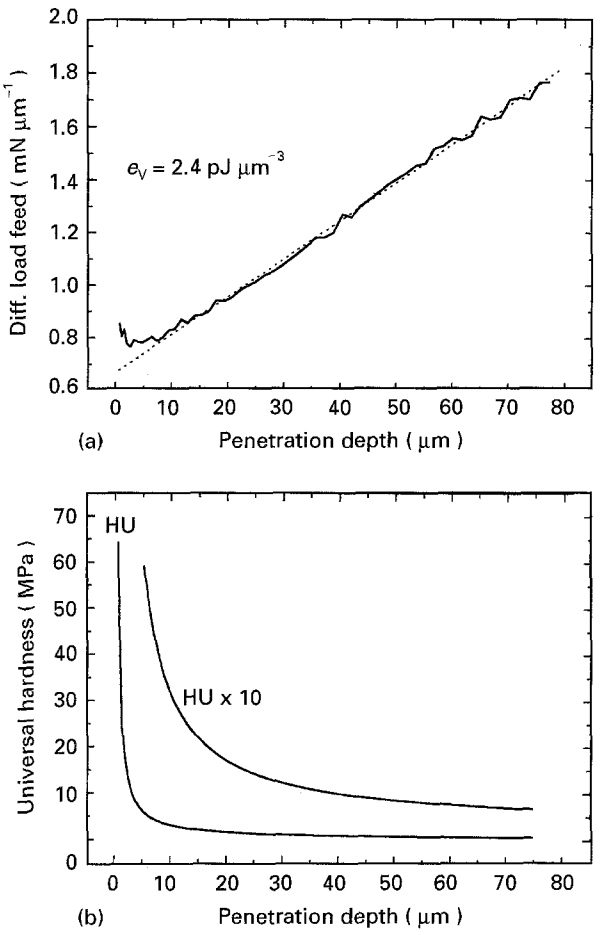

Figure 5 Load–indentation results of India-rubber, end load 100 mN. (a) DLF plot, (----) regression line; (b) HU plot.

TABLE I Three-point characterization of the HU decrease versus penetration depth

Sample material	Figure	s_r [a] (µm)	$s_{1/2}$ [b] (µm)	$s_{1/3}$ [b] (µm)
Alumina	2b	0.08	0.34	0.8
Acryl glass	3b	0.2	0.9	4
Paint	4b	0.2	0.6	2
India-rubber	5b	11	23	40

[a] s_r is the reference penetration depth.
[b] $s_{1/2}$, $s_{1/3}$ are the penetration depths at which the HU value at s_r is decreased to the indexed value.

the indentor. That area, A_r, is then applied instead of the ideal contact area, A_i, obtained from the penetration depth for the hardness calculation. Tip rounding of Vickers indentors is commonly expected in the range 0.2–1 µm.

The equations for different tip rounding shapes [3] can be transformed into one expression

$$A_r = A_i\left(1 + \frac{C_1}{s} + \frac{C_2}{s^2}\right) \quad (2)$$

where the constants C_1 and C_2 represent the specific character of tip rounding. The radius, r, of the tip rounding in the different models is related to the constants by $C_1 \propto r$ and $C_2 \propto r^2$. Starting from the hardness formula $HU = F/A_r$, we obtain

$$F = HU\,A_r$$
$$= HU\,C_i s^2 + \tilde{C}_1 s + \tilde{C}_2 \quad (3)$$

with the shape factor of the ideal indentor, C_i, and the constants $\tilde{C}_1$ and $\tilde{C}_2$.

The proportionality of $\tilde{C}_1$ and $\tilde{C}_2$ in relation to r is the same as for C_1 and C_2. It is interesting to note that Equation 3 leads to the same character of dF/ds, as is obtained from the energetic approach on which Equation 1 is based. Different tip roundings, typical for different indentors of one type, can be derived from both approaches to effect only the absolute term of the DLF plot, while its slope remains constant [10].

Critical remarks on the tip rounding approach should, however, be added.

1. The penetration depth range effected by the ISE is, for the materials investigated here, extended over nearly two orders of magnitude which cannot be declared by the given identical tip rounding of the indentor. In consequence, additional material-dependent parameter(s) have to be introduced, which complicates the model and the calculations.

2. The approach provides no access to the experimentally proved separation between coating and substrate properties [8, 12] and to the evaluation of interface strength [12–14].

Hence, summarizing, the DLF analysis of load–indentation measurements provides a simple means for the calculation of specific energetic material parameters which indicate, in the case of their constancy, a constant resistance of the sample material against the penetration of an indentor.

6. Conclusions

Load–indentation measurements were performed on alumina, acryl glass, colour paint and India-rubber samples. The obtained data were evaluated in terms of the energy-related DLF analysis and in terms of the conventional hardness under load, HU.

The DLF plots proved the constancy of two indentor-specific energy densities in the probed material over extended penetration depth ranges. The slope of the linear ranges is thus suitable for material characterizations. On the other hand, the commonly calculated HU plots of load–indentation measurements require extended and material-specific correction procedures, to equalize the ISE which presently limits the application of load–indentation measurements.

The advantages of DLF analysis as an alternative to the HU calculation, is still limited by the measurement facilities presently available. A more fitted design of the arrangement and of the measurement procedure to the requirements of numerical differentiation can be expected to increase the reliability of the calculated data drastically.

References

1. D. DENGEL, *Materialprüfung* **32** (1990) 310.

2. H. LI, A. GHOSH, Y. H. HAN and R. C. BRADT, *J. Mater. Res.* **8** (1993) 1028.
3. J. M. OLAF, Thesis, Albert-Ludwigs-Universität Freiburg, Germany (1992) in German.
4. W. WEILER and H.-H. BEHNCKE, *Materialprüfung* **32** (1990) 301.
5. M. F. DOERNER and W. D. NIX, *J. Mater. Res.* **1** (1986) 601.
6. P. GRAU and G. BERG, *Materialprüfung* **6** (1994) 227.
7. W. C. OLIVER and G. M. PHARR, *J. Mater. Res.* **7** (1992) 1564.
8. B. ROTHER and D. A. DIETRICH, *Phys. Status Solidi (a)* **142** (1994) 389.
9. D. A. DIETRICH and B. ROTHER, *Materialprüfung*, **37** (1995) to be published.
10. B. ROTHER, *Materialprüfung Werkstoff.*, **26** (1995) 477–482.
11. B. ROTHER and D. A. DIETRICH, *Metalloberfläche* **48** (1994) 758.
12. *Idem, Thin Solid Films* **250** (1994) 181.
13. B. ROTHER, T. LUNOW and G. LEONHARDT, *Surf. Coat. Technol.*, **71** (1995) 229.
14. B. ROTHER, and D. A. DIETRICH, *Materialprüfung* **37** (1995) 30.
15. B. ROTHER, *Materialwiss. Werkstoff.*, **26** (1995) 362.
16. D. A. DIETRICH, Development report 10/93, Ingenieurbüro Dr Dietrich, Burkhardtsdorf, (1993) in German.

Received 6 February
and accepted 7 June 1995